Bull. Mater. Sci., Vol. 36, No. 5, October 2013, pp. 845–852. © Indian Academy of Sciences.

Optimum synthesis conditions of nanometric $Fe_{50}Ni_{50}$ alloy formed by chemical reduction in aqueous solution

MARWA A MOHAMED*, AZZA H EL-MAGHRABY, MONA M ABD EL-LATIF and HASSAN A FARAG†

Department of Fabrication Technology, Advanced Technology and New Materials Research Institute, City of Scientific Research and Technological Applications, New Borg El-Arab, Alexandria 21934, Egypt

†Department of Chemical Engineering, Faculty of Engineering, Alexandria University, Alexandria 21544, Egypt

MS received 2 May 2012; revised 6 July 2012

Abstract. **In the present article, various nanometric $Fe_{50}Ni_{50}$ alloys were synthesized by chemical reduction of the corresponding metal ions, with hydrazine in an aqueous solution. Process variables of reaction temperature, pH of the hydrazine solution and concentration of metal ions were varied in order to determine the optimum synthesis conditions regarding quality, productivity and cost. It is found that pH of hydrazine solution, at low concentration of metal ions, is the most crucial variable affecting the reaction rate, average crystallite and particle sizes of the synthesized nanometric $Fe_{50}Ni_{50}$ alloy, followed by the total concentration of metal ions. Thus, increase of pH of hydrazine solution acts as an efficient stabilizer in reducing the particle size. On the contrary, at high concentration of metal ions, the structural characteristics of the nanometric $Fe_{50}Ni_{50}$ alloy are almost insensitive to reaction temperature and pH of hydrazine solution, but the reduction rate is remarkably sensitive to reaction temperature. Based on these results, it is decided that a reaction temperature of 80 °C, pH of the hydrazine solution of 12·5 and concentration of metal ions of 0·6 M represent the optimum synthesis conditions. The role of pH of hydrazine solution in reducing the alloy's average particle size as well as efficient stabilizer confirms tremendous effect of synthesis conditions on the alloy structure and therefore, the importance of this study for industrial production of nanometric $Fe_{50}Ni_{50}$ alloy.**

Keywords. **FeNi alloys; nanocrystalline alloy; nanoparticles; chemical synthesis; structural characterization.**

1. Introduction

Nanocrystalline metals, with grain sizes typically ranging from 2 to 100 nm, have received worldwide attention, due to their unique optical, electronic, magnetic, chemical and mechanical properties (Koch *et al* 1999; Weertman *et al* 1999; Fan *et al* 2005). Also, metal nanoparticles, exhibiting novel characteristics ascribed to the extremely small dimensions, have received sufficient interest (Petit *et al* 1999; Link and Wang 2000; Lu *et al* 2000). Unusual properties of the nanometric metals that are often superior to those of their larger counterparts resulted in attractive application prospects in many technological areas such as electronics, catalysis, chemical sensors, electromagnetic devices, magnetic data storage, biological and structural applications (Lodder 1996; Sellmyer *et al* 1999; Moreno-Manas and Pleixates 2003; Tartaj *et al* 2003). Investigations have indicated that when a metal is associated with another metal in bimetallic or alloy form, the properties of resulting material could be enhanced with respect to those of the pure metals (Bautista *et al* 1996; Li *et al* 1998). Therefore, a great deal of research has been devoted to the study of nanometric alloys (Enio Lima *et al* 2003a, b; Feng and Zhang 2006; Noskova 2007).

Fe–Ni alloys are considered to be of great importance for various technological applications because of their high saturation magnetization, low coercivity, good anticorrosion properties (Enio Lima 2003a, b), low thermal expansion and excellent mechanical properties (Yeh *et al* 2004). They also have many anomalies of physical properties such as invar (Kumar *et al* 1998) and permalloy (Jen *et al* 1995). These distinctive characteristics are greatly improved when the alloy is synthesized in nanosize range. For example, nanocrystalline Ni–20% Fe alloy is four times stronger than its coarse-grained counterpart. Thus, the compression strength of nanocrystalline Ni–20% Fe alloy at ambient temperature is ≈2200 MPa as compared to ≈ 600 MPa for coarse-grained Ni–20% Fe alloy (Li *et al* 2008). Various synthesis techniques have been developed for the production of nanocrystalline Fe–Ni fine powder, composed of either nanosized particles (size $\leq$ 100 nm) or submicron-sized (100 nm $<$ size $<$ 1 μm) particles, including mechanical alloying (Baldokhin *et al* 1999; Jartych *et al* 2000), hydrogen reduction of metal chlorides (Suh *et al* 2006), chemical reduction in aqueous solution (Enio Lima 2003a, b, 2005; Wei *et al* 2006; Lu *et al* 2007), chemical reduction in aqueous solution combined with hydrogen reduction (Enio Lima 2003a, b) and polyol process-based chemical reduction (Kodama *et al* 2010).

*Author for correspondence (mmohamed@mucsat.sci.eg, marwa945@yahoo.com)

Among these, chemical reduction in aqueous solution is the simplest and has been proved to be an effective economical way for high-yield synthesis of nanocrystalline Fe–Ni nanoparticles. Thus, it can be of great potential in the mass production of such materials. Few researches have been reported on the synthesis of nanometric Fe–Ni alloys by chemical reduction in aqueous solution. However, influence of the synthesis conditions on the nanostructure of nanometric Fe–Ni alloys formed by this method has not been investigated yet to date, although physical and chemical properties of a material are strongly structure dependent, which, in turn, is greatly dependent on conditions of the synthesis process.

In the present work, nanocrystalline $Fe_{50}Ni_{50}$ nanoparticles were synthesized by chemical reduction of the corresponding metal ions in aqueous solution. The most commonly used reducing agents such as borohydride or sodium hypophosphite have been discarded to avoid contamination of the alloy by boron or phosphorus (Simpson 1985; Djokic 1997). Instead, hydrazine was used because it can act as a powerful metal reductant where nitrogen gas and water are the only by-products of the reaction, an important consideration when impurities are to be minimized.

The study was carried out as follows. First, reaction temperature, pH value and concentration of metal ions were manipulated through some preliminary experiments to estimate the synthesis conditions at which the mass production of nanocrystalline $Fe_{50}Ni_{50}$ nanoparticles is logically supposed to be at a minimum cost. Then, the effect of process variables on the reaction rate, alloy composition, crystallite and particle sizes of the prepared samples was further investigated to determine the optimum synthesis conditions.

2. Experimental

2.1 *Materials*

The chemicals used in the synthesis process were nickel chloride hexahydrate ($NiCl_2{\cdot}6H_2O$, 98%) and ferrous chloride ($FeCl_2$, 99%) as sources of metal ions, hydrazine hydrate ($N_2H_4{\cdot}H_2O$, 99%) as a reducing agent, sodium hydroxide (NaOH, 99%) as a catalyst and distilled water as a solvent. $NiCl_2{\cdot}6H_2O$ and $N_2H_4{\cdot}H_2O$ were purchased from Panreac Quimica, Spain. $FeCl_2$ and NaOH were obtained from Spectrum Chemical Mfg. Corp, USA and El Nasr Pharmaceutical, Egypt, respectively.

2.2 *Synthesis process*

The typical synthesis of the nanocrystalline $Fe_{50}Ni_{50}$ fine powder is as follows. Appropriate amounts of $FeCl_2$ and $NiCl_2{\cdot}6H_2O$ were dissolved in distilled water to form aqueous solution of Fe^{2+} and Ni^{2+} ions. Molar ratio of Fe^{2+}/Ni^{2+} was 1:1. The prepared solution was vigorously stirred and heated to an appropriate temperature on a magnetic stirrer equipped with a heating unit. Then, a second solution of aqueous hydrazine, $N_2H_4{\cdot}H_2O$ (50 wt%) and aqueous NaOH (0·1 M) was added to the first solution. The volumetric ratio of aqueous $N_2H_4{\cdot}H_2O$/NaOH solutions was $\approx$ 5:1. Addition of aqueous NaOH was necessary because, in alkaline conditions, hydrazine works as a much better reducing agent than in acidic conditions. This can be deduced from the standard electrode potentials, viz. −0·23 and −1·16 V, for the electrode reactions of hydrazine, $N_2H_4 \leftrightarrow N_2 + 4H^+ + 4e$ and $N_2H_4 + 4OH^- \leftrightarrow N_2 + 4H_2O + 4e$, in acidic and alkaline solutions, respectively (Yu *et al* 2003). The lower the standard electrode potentials, the easier the substances are to be oxidized; in other words, they are simply better reducing agents (http://en.wikipedia.org/wiki/Standard_electrode_potential#Calculation_of_standard_electrode_potentials (Last accessed April 2012)). The molar ratio of hydrazine to metal ions was significantly higher than the stoichiometric one to accelerate the reduction and ensure complete conversion of metal ions to metal atoms. Accordingly, the reaction rate became independent of hydrazine concentration in the reaction solution (5·3 M) and, in turn, only a function of metal ions concentration, reaction temperature and pH value. The precipitation of fine black particles was the result of reduction reaction. The final resulting black particles were separated magnetically, washed repeatedly with distilled water until neutral pH and dried in vacuum at 35 °C for 2 days.

Process variables of reaction temperature (T_R), pH of the hydrazine solution (pH_Z) and total concentration of metal ions (C_M) were varied in order to determine the optimum synthesis conditions of nanocrystalline $Fe_{50}Ni_{50}$ nanoparticles, regarding quality, productivity and cost.

2.2a *Preliminary experiments*: T_R, pH_Z and C_M were manipulated to estimate the synthesis conditions at which the mass production of nanocrystalline $Fe_{50}Ni_{50}$ nanoparticles is logically supposed to be at a minimum cost. Cheapest synthesis requires minimization of the reaction temperature and pH value to save thermal and chemical energies and maximization of the concentration of metal ions to minimize the size of the reaction tank and therefore, capital costs. Also, fair reaction rate is one of the most important requirements to reduce cycle time and improve productivity. Therefore, T_R and pH_z were manipulated (keeping C_M constant at 0·2 M, $[Fe^{2+}] = [Ni^{2+}] = 0{\cdot}1$ M) to determine the minimum values at which the formation of nanocrystalline $Fe_{50}Ni_{50}$ nanoparticles will be completed within about 30 min. C_M was fixed at this low value because lower concentration of metal ions is useful for preparing nanometric metals and alloys. Thereafter, such variables were kept at their minimum values, when C_M was increased to determine the maximum value at which the formation of nanocrystalline $Fe_{50}Ni_{50}$ nanoparticles will be completed within about 30 min.

2.2b *Subsequent investigations*: By changing T_R, keeping pH_Z constant at its minimum value and *vice versa*, a series of samples were prepared. C_M was kept at its maximum value

Table 1. Investigated experimental conditions for optimum synthesis of nanocrystalline $Fe_{50}Ni_{50}$ nanoparticles.

Experiment no.	T_R (°C)	pH_Z	C_M (M)
	Preliminary experiments		
A	60	12	0·2
B	80	11	0·2
C	70	11·5	0·2
D	70	12	0·2
E	70	12·5	0·2
F	70	12·5	0·4
G	70	12·5	0·6
H	70	12·5	0·8
	Subsequent investigations		
I	80	12·5	0·6
J	90	12·5	0·6
K	70	13	0·6
L	70	13·5	0·6

in all the experiments. The experimental conditions in both stages are summarized in table 1.

In some experiments, the reduction reaction started instantaneously, a very rapid expansion with an extremely high gas evolution and precipitation of fine black particles occurred. In others, a green suspension was formed at the beginning then its colour was turned to dark brown and finally the fine black particles were formed.

2.3 *Characterization*

X-ray diffraction (XRD) was employed to characterize the crystallographic texture, grain (crystallite) size and lattice parameter of the synthesized black particles. XRD measurements were carried out on a Shimadzu XRD-7000 diffractometer (30 kV, 30 mA; CuKα + Ni-filtered radiation, λ = 0·15406 nm). The 2θ range was 30–110°, at a scanning rate of 4°/min and a scanning step of 0·018°.

The morphology and particle sizes were analysed by scanning electron microscopy (SEM, JEOL, Model JSM 6360 LA, Japan) operating at 20 kV. SEM samples were prepared by dropping a diluted dispersion of particles onto a glass slide and letting the solvent to evaporate. Chemical compositions were estimated by an area analysis using energy dispersive X-ray spectroscopy (EDS) system equipped with SEM.

3. Results and discussion

A possible mechanism of formation of Fe–Ni alloy may be as follows. During heating aqueous solution of Fe^{2+} and Ni^{2+} ions, a portion of Fe^{2+} was replaced by Fe^{3+}, owing to the ease of oxidation of Fe^{2+} to Fe^{3+}, which is promoted by heat. In experiments A and B, a yellowish green suspension was formed on contact between the hydrazine solution and the metal salt solution. Then, the colour of the suspension turned to dark brown after about 5 min. However, no reduction reaction occurred and, as a result, the black Fe–Ni particles were not formed even after 1 h. The yellowish green suspension indicates the formation of ferrous, ferric and nickel hydroxides at the beginning of the process, according to the following reactions:

$$FeCl_2 + 2NaOH \rightarrow Fe(OH)_2 + 2NaCl, \quad (1)$$

$$FeCl_3 + 3NaOH \rightarrow Fe(OH)_3 + 3NaCl, \quad (2)$$

$$NiCl_2 + 2NaOH \rightarrow Ni(OH)_2 + 2NaCl. \quad (3)$$

Then the formed hydroxides were decomposed with heat into their dark brown oxides as follows:

$$Fe(OH)_2 \xrightarrow{\text{Heat}} FeO + H_2O, \quad (4)$$

$$2Fe(OH)_3 \xrightarrow{\text{Heat}} Fe_2O_3 + 3H_2O, \quad (5)$$

$$Ni(OH)_2 \xrightarrow{\text{Heat}} NiO + H_2O. \quad (6)$$

The formed oxides, however, were not further reduced by hydrazine to metal atoms because values of the operating T_R in experiment A and the pH_Z in experiment B were too low to provide the required energy to drive the reaction within the allowed period of time. The reduction reaction scheme can be expressed by the following equations:

$$2N_2H_4 + 8OH^- \leftrightarrow 2N_2 + 8H_2O + 8e^-, \quad (7)$$

$$Fe^{3+} + e^- \rightarrow Fe^{2+}, \quad (8)$$

$$Fe^{2+} + Ni^{2+} + 4e^- \rightarrow FeNi. \quad (9)$$

According to the law of mass action, the electrode reaction of hydrazine will tend to proceed to the right, and as a result, the rate of reduction reaction increases when the concentration of $[OH^-]$ ions increases. Also, it is revealed from previous works (Chen and Hsieh 2002; Yang *et al* 2004) that an elevated reaction temperature is quite helpful in accelerating the reduction rate of iron and nickel ions. Therefore, the operating T_R and the amount of aqueous NaOH added to the hydrazine solution for adjusting the pH_Z were increased slightly in experiment C. The reduction reaction started after about 7 min and precipitation of fine black particles occurred. The reaction appeared to have been completed within about 20 min.

Figure 1 shows XRD pattern of the resultant particles (curve b). For comparison, XRD patterns of the resultant particles when the molar ratio of Fe^{2+} to Ni^{2+} in the reaction solution was 100:0 (curve a) and *vice versa* (curve c) are also displayed. According to the database of International Centre of Diffraction Data (ICDD), the diffraction peaks in curve a (2θ = 35·6, 43, 56·9 and 62·6°) match the (311), (400), (511) and (440) characteristics of cubic magnetite (Fe_3O_4),

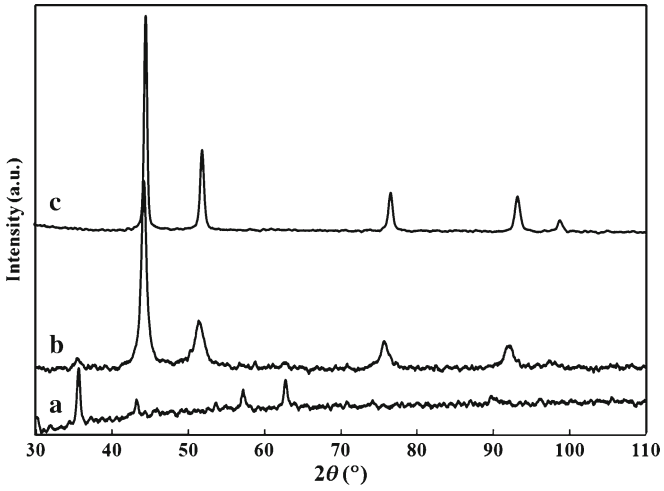

Figure 1. XRD patterns of resultant particles synthesized at different Fe^{2+}/Ni^{2+} ratios in starting reaction solutions: (**a**) 100:0; (**b**) 50:50 and (**c**) 0:100.

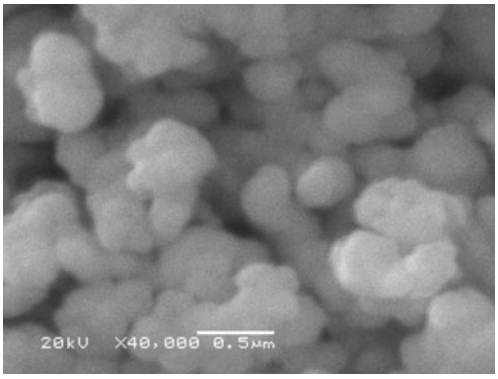

Figure 2. SEM image of $Fe_{50}Ni_{50}$ alloy prepared in experiment C.

but not Fe atoms (ICDD card 00-001-1111). This is probably due to two reasons: (i) when only Fe^{2+} existed in the starting reaction solution, large portions of Fe^{2+} ions were oxidized to Fe^{3+} ions, which were then partially reduced to $Fe^{8/3+}$, forming Fe_3O_4 and (ii) the Fe atoms resulting from complete reduction of the other portion of Fe^{2+} were oxidized during washing and drying to Fe_3O_4, owing to the ease of Fe oxidation. On the contrary, the five characteristic peaks for face-centred cubic (fcc) nickel (2θ = 44·5, 51·9, 76·4, 93 and 98·8°), marked by Miller indices ((111), (200), (220), (311) and (222)) are observed in curve c (ICDD card 00-001-1258). This reveals that the resultant particles, when the molar ratio of Fe^{2+} to Ni^{2+} was 0:100, are pure fcc nickel. The observable XRD peaks in curve b (2θ = 44·1, 51·4, 75·7, 91·7 and 97·5°) are attributed to the disordered fcc γ-Fe–Ni taenite phase (ICDD card 00-038-0419). Only a very weak peak (2θ = 35·4°) for magnetite can also be detected. The absence of XRD peaks, characteristics of α-Fe (i.e. at 2θ of 65·2°) and (fcc)-Ni, indicates that no iron or nickel was formed. In addition, no iron oxides or nickel oxides can be detected in the XRD pattern. This reveals that the resultant particles are mainly pure Fe–Ni alloy, when the ratio of Fe^{2+} to Ni^{2+} was 50:50 (1:1).

Lattice parameters, a, of the fcc Ni and Fe–Ni samples produced, are calculated from the following relationship:

$$a_{\text{fcc}} = \sqrt{3} d_{111}, \tag{10}$$

where d_{111} is the measured average atomic plane spacing of the (111) planes for each sample.

The lattice parameter of the fcc Fe–Ni alloy (3·553 Å) is between those of pure fcc nickel (3·519 Å) and fcc iron (3·588 Å) (Abrahams *et al* 1962) and is in agreement with the previously reported value for $Fe_{50}Ni_{50}$ alloy (Enio Lima *et al* 2005). On the other hand, EDS quantitative analysis results in the composition of 47 at.% Fe and 53 at.% Ni, excluding the other elements such as carbon for supporting film and oxygen for the thin oxide layer on particle surface. XRD peaks, lattice parameter and compositional data from EDS system agree well with each other, indicating that the precipitated particles in experiment C are mainly pure $Fe_{50}Ni_{50}$ alloy.

The average crystallite size of the $Fe_{50}Ni_{50}$ alloy produced, which is calculated from the full width at half maximum of the (111) peak in the XRD pattern using Scherrer formula (Cullity 1956) is 12·5 nm. Nevertheless, the SEM image, presented in figure 2, shows that the $Fe_{50}Ni_{50}$ alloy produced is composed of spherical particles with a mean diameter of about 212 nm. This suggests that each spherical particle is nanostructured, i.e. it is composed of several nanocrystallites, as previously evidenced earlier (Enio Lima *et al* 2003a, b, 2005; Wei *et al* 2006). Considering both XRD and SEM results, it is concluded that the prepared $Fe_{50}Ni_{50}$ alloy is composed of nanocrystallites but not nanoparticles.

The value of pH_Z was increased to 12 in experiment D. The rate of reduction reaction increased, the reaction started after about 5 min and appeared to have been completed in 15 min. The chemical composition of the produced alloy is 46 at.% Fe and 54 at.% Ni. The average crystallite size, as estimated from the corresponding XRD pattern, decreases down to 8 nm. Furthermore, the SEM image, presented in figure 3, shows that the produced alloy is composed of much smaller spherical particles with a mean diameter of about 147 nm, compared with that produced from experiment C. This reveals that stronger alkalinity of the reaction solution due to increased pH_Z efficiently restricts the growth of $Fe_{50}Ni_{50}$ particles. The mechanism of formation of the $Fe_{50}Ni_{50}$ particles may be as follows. At the beginning, few nuclei containing Fe and Ni atoms were formed. Then, more metal atoms were reduced and adsorbed on the nuclei, forming crystals. Finally, the crystals aggregated into larger spherical particles. Strong alkalinity of the reaction solution is useful for preparing tinier alloy particles, probably because this made $Fe(OH)_2$ and $Ni(OH)_2$ suspension, formed at the beginning of the synthesis process, negatively charged. This may be because free OH^- ions in the solution wrapped the hydroxides suspension and therefore, became spherical micelles. As a result, the alloy nucleated later in the

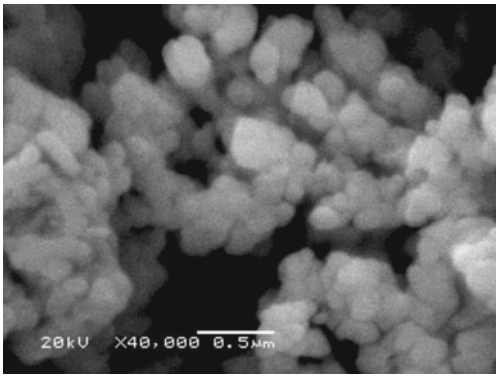

Figure 3. SEM image of $Fe_{50}Ni_{50}$ alloy prepared in experiment D.

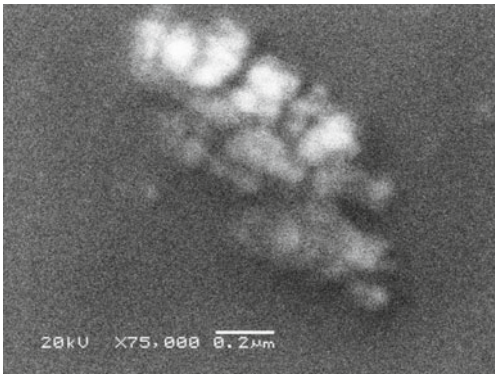

Figure 5. SEM image of $Fe_{50}Ni_{50}$ alloy prepared in experiment F.

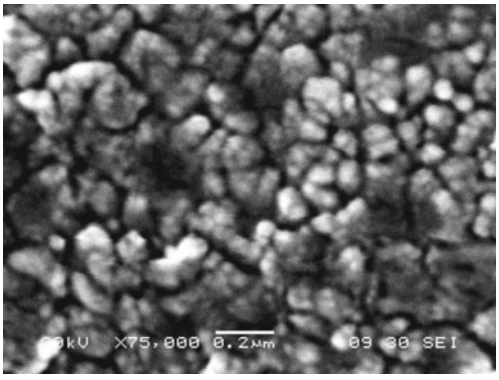

Figure 4. SEM image of $Fe_{50}Ni_{50}$ alloy prepared in experiment E.

micelles, which are capable of preventing excess aggregation of crystals and subsequently the growth of $Fe_{50}Ni_{50}$ particles.

Accordingly, the value of pH_Z was further increased to 12·5 in experiment E, in order to prepare tinier particles. Again, rate of reduction reaction increased, the reaction started immediately and continued for about 10 min. The chemical composition of the produced alloy is 48 at.% Fe and 52 at.% Ni. The average crystallite size remains the same at 8 nm, whereas the average particle size, which is determined from the SEM image (figure 4), significantly decreases to about 56 nm, i.e. the produced alloy is composed of spherical nanoparticles.

At this point it is worth mentioning that the earlier results interestingly reveal that the increase of pH_Z acts as an efficient stabilizer in reducing the particle size of $Fe_{50}Ni_{50}$ alloy. This is considered a new important finding. Thus, the previous researches reported on the synthesis of nanometric $Fe_{50}Ni_{50}$ alloys by chemical reduction in aqueous solution indicated that the average crystallite and particle sizes of $Fe_{50}Ni_{50}$ synthesized in the presence of stabilizers were 9 nm and 70 nm as compared to 15 nm and 96 nm for the corresponding alloy synthesized in the absence of stabilizer (Enio Lima *et al* 2003a, b, 2005; Wei *et al* 2006).

For determining the maximum concentration of metal ions at which the formation of nanocrystalline $Fe_{50}Ni_{50}$ nanoparticles will be compeleted within 30 min at the most, C_M was increased by a step of 0·2 M up to 0·8 M in experiments F, G and H, respectively. The reduction rate decreased as C_M increased. Thus, no reduction occurred at $C_M = 0{\cdot}8$ M even after 1 h (experiment H). For experiments F and G, the reduction reaction started immediately or after 10 min and continued for about 10 min or 30 min, respectively. The contents of iron in the resultant Fe–Ni alloys are 45 and 47 at.%, respectively. Average crystallite sizes are 9 nm and 10·5 nm. Average particle sizes, as detected from the SEM micrographs (figures 5 and 6a), are 66 nm and 97 nm. This clearly indicates that the average crystallite and particle sizes of the Fe–Ni alloy are increased with increasing total concentration of metal ions. This may be because when the concentration of metal ions increases, the formation of $Fe(OH)_2$ and $Ni(OH)_2$ is accelerated, and more OH^- ions is consumed in the reaction. As a result, the number of free OH^- ions in the solution and therefore, the rate of reduction reaction will decrease and less Fe–Ni nuclei will be formed. With less Fe–Ni nuclei being formed, the growth rates of the nuclei will increase and consequently large crystals will form. The large crystals will then grow into large particles for two possible reasons: (a) with the decreased number of free OH^- ions in the solution, the $Fe(OH)_2$ and $Ni(OH)_2$ suspensions will not be well wrapped with the free OH^- ions. This increases the opportunities for the crystals to aggregate into large spherical particles; (b) with higher concentrations of metal ions, the total number of metal atoms that are reduced and adsorbed on the nuclei will be increased, so that larger crystals will be formed, which, in turn, will aggregate into larger sphere particles.

Based on the precedent results, T_R of 70 °C, pH_Z of 12·5 and C_M of 0·6 M can be considered to represent the synthesis conditions at which the mass production of nanocrystalline $Fe_{50}Ni_{50}$ nanoparticles is logically supposed to be at a minimum cost.

To attain the optimum synthesis conditions of nanocrystalline $Fe_{50}Ni_{50}$ nanoparticles, different values of T_R and

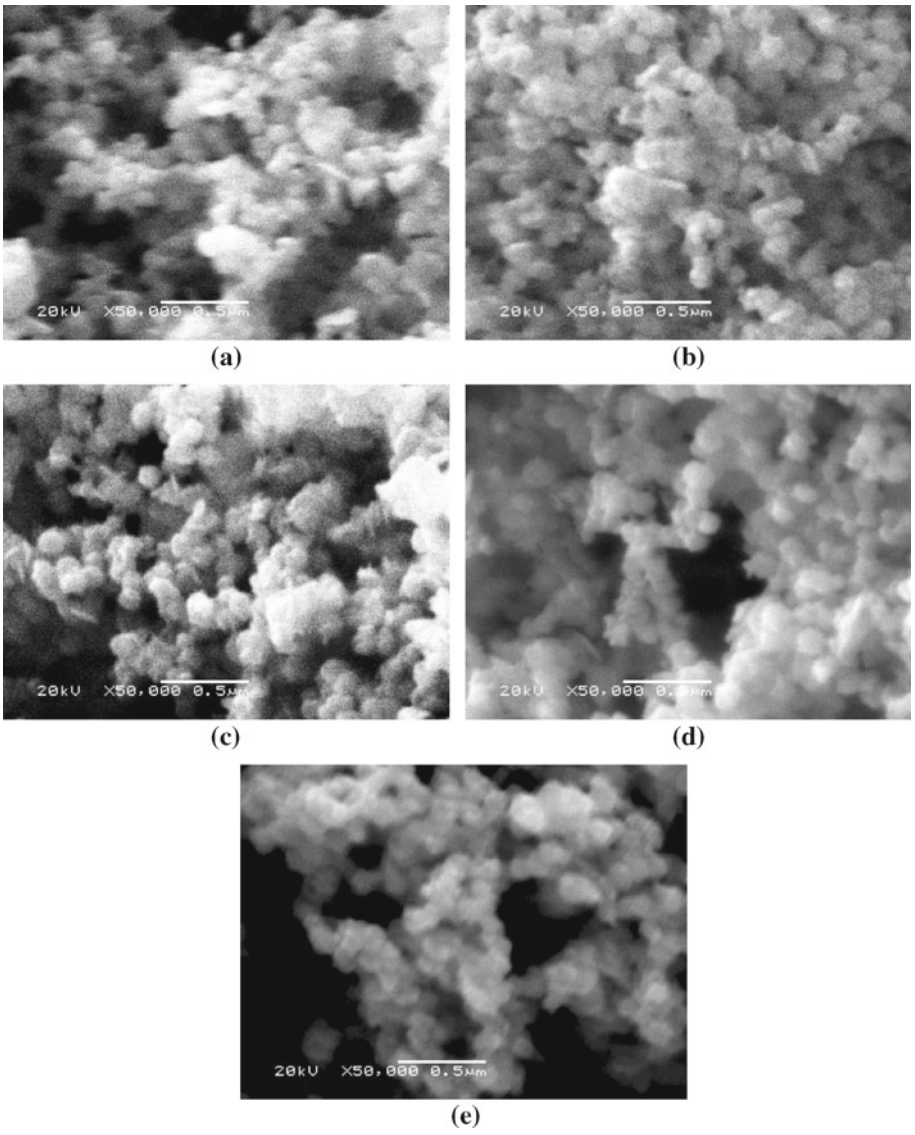

Figure 6. SEM images of $Fe_{50}Ni_{50}$ alloys prepared in (**a**) experiment G; (**b**) experiment I; (**c**) experiment J; (**d**) experiment K and (**e**) experiment L.

pH_Z were used in experiments I–L, as shown in table 1. Table 2 shows variation of the alloy composition, crystallite size and reaction completion time with experimental conditions. Additionally, SEM images of the prepared alloys with respect to different experimental conditions are presented in figure 6(a–e). It is noteworthy that the alloy composition does not follow any specific trend as the experimental conditions are changed, indicating that it is not affected by the variation of experimental conditions. In contrast, the crystallite size decreases as T_R or pH_Z increases. The increase of T_R and pH_Z accelerate the reduction rate and more Fe–Ni nuclei are formed. With more Fe–Ni nuclei being formed, the growth rates of the nuclei get lower and consequently tinier crystals are formed.

It appears that the average particle size is not significantly affected by the variation of experimental conditions. SEM images show that the sizes of $Fe_{50}Ni_{50}$ nanoparticles do not change significantly, when T_R or pH_Z are increased. The effect of reaction temperature on the particle size may be explained by considering two competing aspects: first, the size of $Fe_{50}Ni_{50}$ crystals decrease with the increase of T_R, leading to the decreasing size of $Fe_{50}Ni_{50}$ nanoparticles. Second, the higher temperature intensifies the collision and coalescence of $Fe_{50}Ni_{50}$ crystals, which enhances the opportunities for the crystals to aggregate into larger particles. Therefore, size of $Fe_{50}Ni_{50}$ nanoparticles is not simply increased or decreased with the increase of the reaction temperature. Invariability of particle size with the increase of pH_Z implies that the increased free OH^- ions are relatively low as compared with the amount of $Fe(OH)_2$ and $Ni(OH)_2$ particles at high concentration of metal ions. Therefore, they do not contribute to the formation of many more micelles, and as a result, the particle size does not significantly decrease with the increase of pH_Z.

Table 2. Reaction time, chemical composition and crystallite size of nanocrystalline $Fe_{50}Ni_{50}$ alloys prepared at different experimental conditions.

	Chemical composition		Crystallite size	Delay time	Reaction time
Experiment no.	at.% Fe	at.% Ni	(nm)	(min)	(min)
G	47	53	10·5	10	30
I	46·5	53·5	10	5	15
J	46	54	9·5	Immediately	10
K	47	53	10	10	30
L	45	55	9	10	25

Although the characteristics of the prepared alloys at different experimental conditions are rather similar, the reaction time is significantly affected by the increase of the reaction temperature. It can be noted that for every 10 °C increase in T_R, the reaction time decreases to half. This implies that the synthesis conditions applied in experiment I (T_R of 80 °C, pH_Z of 12·5 and C_M of 0·6 M) represent the optimum synthesis conditions of the nanocrystalline $Fe_{50}Ni_{50}$ nanoparticles. This is because such conditions, as compared with the cheapest ones, offer much better alloy productivity by reducing the reaction time to half, the quality of the produced alloy is almost the same due to the slight changes in crystallite and particle sizes, meanwhile, the process costs are a little higher due to a small increase in reaction temperature.

4. Conclusions

In this paper, we report the synthesis of nanometric $Fe_{50}Ni_{50}$ alloy via chemical reduction in aqueous solution under different synthesis conditions. The study reveals that T_R of 70 °C, pH_Z of 12·5 and C_M of 0·6 M represent the synthesis conditions at which the mass production of nanocrystalline $Fe_{50}Ni_{50}$ nanoparticles is logically supposed to be at a minimum cost. Whereas at a T_R of 80 °C, same values of pH_Z and C_M represent the optimum synthesis conditions. On the other hand, analyses of results indicate the reduction rate, crystallite and particle sizes of the prepared alloys are greatly affected by the variation of synthesis conditions. A pH_Z at low concentration of metal ions is the most crucial variable affecting them, followed by C_M. The characteristics of the prepared alloys, however, are almost insensitive to T_R and pH_Z at higher concentration of metal ions. Nevertheless, the reduction rate is remarkably influenced by the variation of T_R. Interestingly, the most important new finding of this study is that the increase of pH_Z at low values of C_M acts as an efficient stabilizer in reducing the alloy particle size, indicating that adjusting the synthesis conditions can eliminate the need for expensive stabilizers to restrict the growth of nanometric $Fe_{50}Ni_{50}$ particles. This decides that the synthesis conditions play a critical role in controlling the cost, productivity, structure and therefore, properties of the nanocrystalline $Fe_{50}Ni_{50}$ nanoparticles.

References

Abrahams S C, Guttman L and Kasper J S 1962 *Phys. Rev.* **127** 2052

Baldokhin Yu V, Tcherdyntsev V V, Kaloshkin S D, Kochetov G A and Pustov Yu A 1999 *J. Magn. Magn. Mater.* **203** 313

Bautista F M, Campelo J M and Garcia A 1996 *J. Mol. Catal. A Chem.* **104** 229

Chen D H and Hsieh C H 2002 *J. Mater. Chem.* **12** 2412

Cullity B D 1956 *Elements of X-ray diffraction* (Addison-Wesley Publishing Company, Inc.) Chapter 3, p. 99

Djokic S S 1997 *J. Electrochem. Soc.* **144** 2358

Enio Lima Jr, Drago V, Bolsoni R and Fichtner P F P 2003a *Solid State Commun.* **125** 265

Enio Lima Jr, Drago V, Fichtner P F P and Domingues P H 2003b *Solid State Commun.* **128** 345

Enio Lima Jr, Drago V, Lima J C and Fichtner P F P 2005 *J. Alloys Compd.* **396** 10

Fan G J, Choo H, Liaw P K and Lavernia E J 2005 *Mater. Sci. Eng.* **409A** 243

Feng J and Zhang C-P 2006 *J. Colloid Interf. Sci.* **293** 414

Jartych E, Zurawicz J K, Oleszak D and Pekala M 2000 *J. Magn. Magn. Mater.* **208** 221

Jen S U, Shieh S P and Liou S S 1995 *J. Magn. Magn. Mater.* **147** 49

Koch C C, Morris D G, Lu K and Inoue A 1999 *Mater. Res. Soc. Bull.* **24** 54

Kodama D, Shinoda K, Kasuya R, Tohji K and Doi M 2010 *J. Appl. Phys.* **107** 09A320-09A320-3

Kumar S, Roy K, Maity K, Sinha T P, Banerjee D, Das K C and Bhattacharya R 1998 *Phys. Status Solidi.* **A167** 175

Li Y, Chen J and Qin L 1998 *J. Catal.* **178** 76

Li H, Liawa P K, Chooa H, Tabachnikova E D, Podolskiy A V, Smirnov S N and Bengus V Z 2008 *Mater. Sci. Eng.* **A493** 93

Link S and Wang Z L 2000 *J. Phys. Chem.* **B104** 7867

Lodder J C 1996 *Thin Solid Films* **474** 281

Lu L, Wang L B and Ding B Z 2000 *J. Mater. Res.* **15** 270

Lu X, Liang G and Zhang Y 2007 *Mater. Sci. Eng.* **B139** 124

Moreno-Manas M and Pleixates R 2003 *Acc. Chem. Res.* **36** 638

Noskova N I 2007 *J. Alloys Compd.* **307** 434

Petit C, Cren T and Roditcher D 1999 *Adv. Mater.* **11** 1198

Sellmyer D J, Yu M and Kirby R D 1999 *Nanostruct. Mater.* **12** 1021

Simpson D K 1985 *Met. Fin.* **83** 57

Suh Y J, Jang H D, Chang H, Kim W B and Kim H C 2006 *Powder Tech.* **161** 196

Tartaj P, Morales M P, Veintemillas-Verdaguer S, Gonzalez-Carreno T and Serna C J 2003 *J. Phys. D: Appl. Phys.* **36** 182

Weertman J R, Farkas D, Hemker K, Kung H, Mayo M, Mitra R and Swygenhoven V H 1999 *Mater. Res. Soc. Bull.* **24** 44

Wei X W, Zhu G X, Zhou J H and Sun H Q 2006 *Mater. Chem. Phys.* **100** 481

Yang C, Xing J, Guan Y, Liu J and Liu H 2004 *J. Alloys Compd.* **385** 283

Yeh Y M, Tu G C and Fang T H 2004 *J. Alloys Compd.* **372** 224

Yu K, Kim D J, Chung H S and Liang H Z 2003 *Mater. Lett.* **57** 3992